EFFECT OF CARBONATION CURING ON FIBER-CEMENT PRODUCTS BASED ON MGO-SIO_2 SYSTEMS

GONZALO MÁRMOL, JULIÁN E.M. BALLESTEROS, JULIANO FIORELLI,

HOLMER SAVASTANO JR.

University of Sao Paulo, Faculty of Animal Science and Food Engineering, Department of Biosystems Engineering, Duque de Caxias Norte Street, 225, 13630-000 Pirassununga, SP, Brazil

ABSTRACT

Thin fiber-cement (FC) plates made out of MgO-SiO_2 binding systems and reinforced with polypropylene (PP) and cellulosic (pine) pulp, produced by a slurry-dewatering and pressing technique, were mechanically and physically characterized. Samples were cured under two different conditions: steam water curing at 55ºC and high CO_2 concentration (20% by volume). To evaluate the mechanical performance of the cementitious based material and the possibility to be reinforced for fiber-cement production, 4 point-bending test was used. Also apparent porosity (AP), bulk density (BD) and water absorption (WA) were assessed. In order to study the effects of carbonation on the materials, and their performance over time, cycles of accelerated ageing were used. The analyzed materials showed excellent flexural strength and toughness, which were maintained after ageing. Carbonation helped to increase flexural strength and physical properties, becoming an attractive method to improve fiber-cement products made with this alternative binder.

KEYWORDS:

MgO-based cement; carbonation; matrix densening

INTRODUCTION

Accelerated carbonation has been shown to be capable of improving cementitious matrices for fiber cement (FC) application (Almeida et al., 2013; Pizzol et al., 2014; Purnell et al., 2001; Santos et al., 2015). The main effect of carbonation on hydrated Portland cement paste is the conversion of portlandite [$Ca(OH)_2$] into calcite and vaterite ($CaCO_3$). This reaction increases the density of the matrix, (Frías and Goñi, 2013; Mo et al., 2015; Morandeau et al., 2015; Zha et al., 2015), making it more rigid and stronger. It also strengthens the fiber-matrix interface, but this can modify the fracture mechanism, often leading to a reduction in the deflection during flexural test, despite significant increases in the modulus of rupture (MOR) and modulus of elasticity (MOE) (Almeida et al., 2013; Pizzol et al., 2014; Purnell et al., 2001; Santos et al., 2015).

Reactive periclase binders can also harden by carbonation, sequestering CO_2 as part of the process of making construction materials (Unluer and Al-Tabbaa, 2015, 2014, 2013; Vandeperre and Al-Tabbaa, 2007). When MgO is carbonated in the presence of water, hydrated magnesium carbonates (HMC) are produced, with general formula $xMgCO_3.Mg(OH)_2.yH_2O$ (Botha and Strydom, 2001; Lanas and Alvarez, 2004). These compounds bind both water and CO_2 and thus create a very large additional solid volume, giving them a much greater potential than Portland cement in terms of overall carbonated binder efficiency. The transformation of brucite into HMC, identically to what occurs for $Ca(OH)_2$ when turns into ($CaCO_3$), increases strength of the hydrated pastes.

Therefore, the aim of this work was to study the behavior of FC elements made out of blends of MgO-SiO_2 reinforced with both polymeric (polypropylene) and lignocellulosic (pine pulps) considering:

- The effects of the early-age carbonation on the cement matrix and the fiber-cement composites,
- The evolution of mechanical and physical properties after accelerated ageing and
- The thermodynamic stability of the possible obtained hydrated magnesium carbonates in the matrix.

MATERIALS AND METHODS

Raw materials and samples production

The formulation of the composites employed in this study is similar to the FC industry parameters for air-cured products, as shown in **Table 1.**

Table 2- Formulation of the fiber-cement samples.

	Raw materials	Amount (% by mass)
Matrix	Magnesium oxide AR 200	42
	Silica Fume Elkem U920	28
	Limestone Itaú	25
Cellulosic pulp	Unbleached pine pulp (CSF = 36)	3
Synthetic fiber	Polypropylene	2

200x200x6mm FC pads were produced at laboratory scale using a slurry vacuum-dewatering process followed by pressing technique, as a laboratorial adaptation of the Hatschek process described in details by Savastano et al. (Savastano Jr. et al., 2000). Pads were wet cut into four 165×40 mm samples for flexural testing. In order to assess the effects of carbonation on FC MgO based samples, 2 types of curing were set as follows in Figure 1.

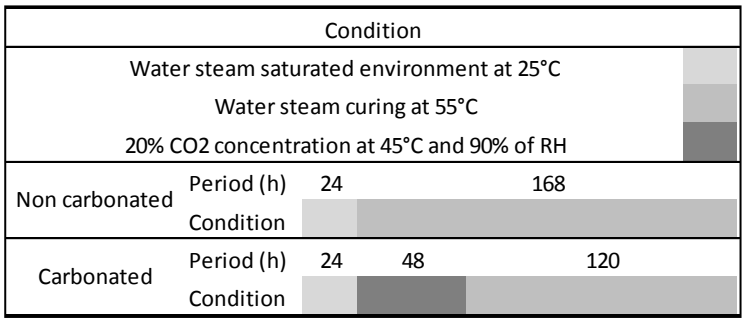

Figure 1- Curing conditions diagram for non-carbonated and carbonated samples

200 Accelerated cycles were used to evaluate the long-term performance of FC. This technique aimed to speed up natural weathering using soaking and drying cycles. Specimens were successively immersed into water at 20 ± 5ºC for 170 min and, after an interval of 10 min, were heated up to 60 ± 5ºC for 170 min in a ventilated oven. Another interval of 10 min at room temperature also preceded the subsequent cycle.

Testing methods

4-point bending tests were performed after different curing conditions with a deflection speed of 5 mm/min. After mechanical testing, aliquots of each sample were crushed and immersed in acetone to stop hydration reactions and later dried at 60ºC. X-ray diffraction and thermogravimetric characterization was performed at different ages. A Horiba LA-960 X-ray diffractometer was set for CuK_{α} radiation at a voltage of 40 kV and a current of 30 mA, between 5-65º with a speed of 10º/min. A Netzch STA 440 F3 Jupiter TG equipment in inert atmosphere of nitrogen was set at a flow rate of 60 mL/min and performed from 25 to 1000ºC at a heating rate of 10ºC/min. Physical properties, apparent porosity (AP), bulk density (BD) and water absorption (WA) were obtained following procedures specified by the ASTM C 1185 Standards (2012)(ASTM C1185-08, 2012). The fractured surfaces of specimens resulting from the mechanical tests were carbon coated and later polished for backscattered electron microscopy (SEM).

RESULTS AND DISCUSSIONS

X-Ray diffraction analysis

X-Ray analysis of the FC composites is displayed in Figure 2. The efficiency of the curing conditions to accelerate carbonation is proven by the reduction in intensity of brucite (B) peaks for carbonated samples, centered at around 18, 38 and 58º 2θ, being further reduced for aged samples. The lower content of B for carbonated samples is related to the presence of new peaks due to the presence of HMC (H), so it is possible to infer the carbonation of $Mg(OH)_2$. Another difference between C and NC samples is that C samples present a reduction of the amorphous halo correspondent to M-S-H gel presence (centered between 32-39º and 53-63º 2θ (Li et al., 2014; Lothenbach et al., 2015; Szczerba et al., 2013; Walling et al., 2015), while the characteristic hump of amorphous SiO_2 is increased. This may be explained by the efficiency of carbonation conditions, where most of brucite is transformed into HMC and only reduced amount is able to react with SiO_2 to form M-S-H gel.

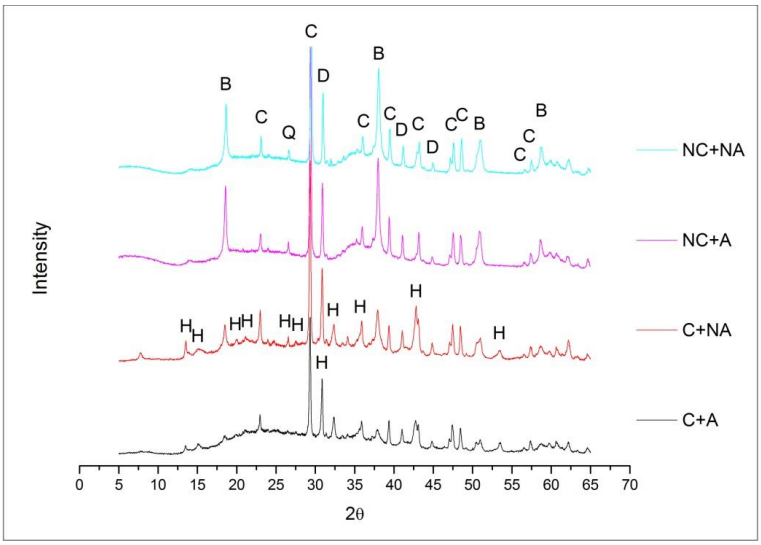

Figure 2- X-Ray diffractograms of the MgO-based FC composites samples submitted to the different treatments: non-carbonated and non-aged (NC+NA), non-carbonated and aged (NC+A), carbonated and non-aged (C+NA) and carbonated and aged (C+A). Peaks marked are brucite (B), calcite (C), quartz (Q), Dolomite (D) and HMC (H).

Thermogravimetric analysis

From DTG curves displayed in Figure 3 , the effect of carbonation curing is proven by the presence of additional mass losses in the C samples, both unaged and aged (C+NA and C+A), unnoticed in NC samples. These mass losses in the temperatures range of (1) 220–290ºC, (2) 375–470ºC and (3) 470-550ºC are related to the dehydration from lattice water, dehydroxylation and decarbonation of HMC respectively (Botha and Strydom, 2001; Haurie et al., 2007; Hollingbery and Hull, 2012, 2010a, 2010b; Vágvölgyi et al., 2008).

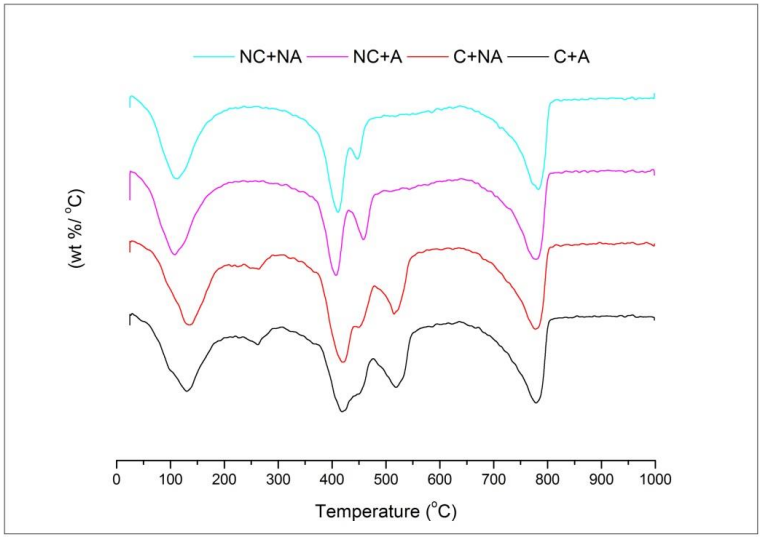

Figure 3- DTG curves of the MgO-based FC composites samples submitted to the different treatments: non-carbonated and non-aged (NC+NA), non-carbonated and aged (NC+A), carbonated and non-aged (C+NA) and carbonated and aged (C+A).

Also from DTG analysis, it is confirmed the stability of HMC formed as a result of the carbonation reaction, since the w.t. % associated to this new phase remains at similar levels before and after ageing. The total area of the C composites due to the mass loss related to HMC decomposition before and after ageing (C+NA and C+A) is 7.82% and 8.09%, respectively. Although there is no statistical significant difference, aged samples (C+A) present a higher amount of HMC, which suggests that wetting-drying cycles are favorable conditions for carbonation with atmospheric CO_2.

Microstructural analysis by Scanning Electronic Microscopy

By means of SEM analysis, it was also established the effectiveness of the high CO_2 concentration curing. Carbonated samples present additional structures unnoticed before carbonation curing Apart from Mg(OH)2 (MH in Figure 4a) and M-S-H gels, rosette shaped crystals are evident (encircled in yellow in Figure 4a and b). In line with different authors (Beall et al., 2013; Chen et al., 2015; Gautier et al., 2014; Li et al., 2003), this morphology is characteristic of hydromagnesite crystals which is described as rosette-like microstructure with crystalline walls interconnected to each other (Figure 4c). Also, the hydromagnesite used for the synthesis of forsterite (Chen et al., 2015) matches the exhibited dimensions to those presented by the crystals of hydromagnesite in Figure 4, with extremely thin sheets of around 20 nm in thickness and less than 1 μm in length.

From Figure 4b, it is noticed a more compacted amorphous structure (marked in white), different from HMC crystals. These particles are hydrated magnesium silicate from the reaction between MgO and amorphous SiO_2 in water and have been satisfactorily used to produce FC composites reinforced only with cellulosic fibers with no degradation effects (Mármol and Savastano, 2017).

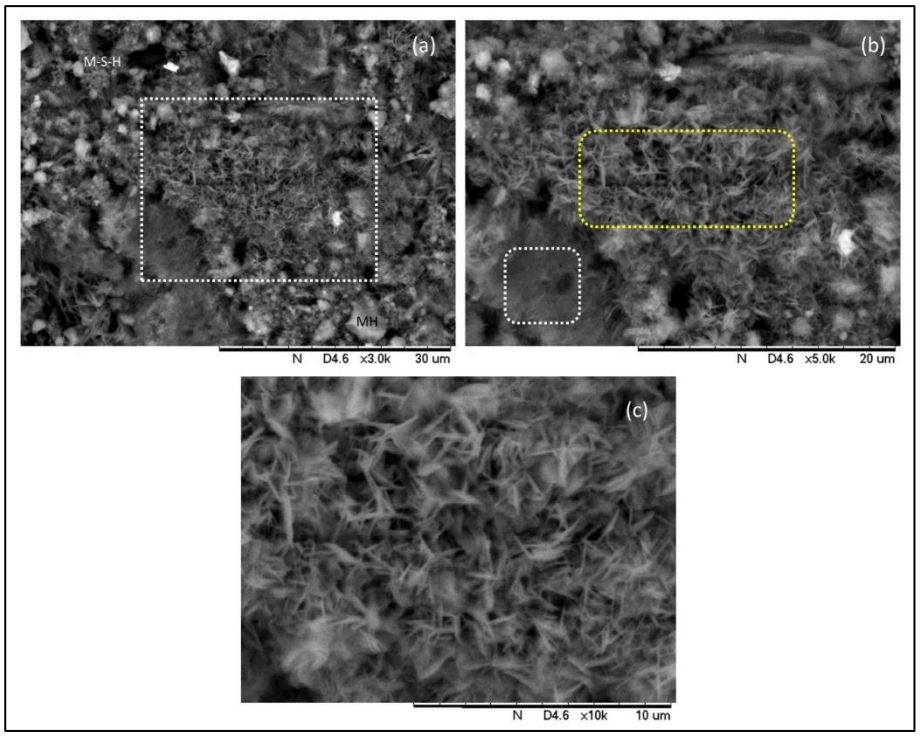

Figure 4- (a) SEM of a fractured surface of a carbonated sample (C+A). The white dashed line squares the zoomed are depicted in (b). The white dashed line shows amorphous M-S-H carbonation and the yellow dashed line is the zoomed area depicted in (c), exhibiting HMC crystals. All images are for aged composites after accelerated aging test.

Mechanical and physical tests

From mechanical results summarized in Table 3, carbonated samples present more rigid matrices than non-carbonated, since MOE and LOP values are far higher. It is also observed that rigidity parameters are increased after ageing for both non-carbonated and carbonated samples. Due to the improvement of the matrix performance, the flexural strength of carbonated samples is also increased, although with no statistical difference is produced. In spite of the lower SD values for carbonated samples, SE energy is similar to the rest of the samples regardless the curing process. The significant reduction of SD values for carbonated samples is related to the modification of the fiber-matrix interface, which is densified because of carbonation reaction. Denser fiber-matrix interfaces yield excessive adherence between matrix and fiber, which is translated into less deformation of the composites since higher loads are transferred to the fibers and pull-out is reduced, producing less progressive collapse of the composite.

Table 3- Mechanical and physical properties of the FC samples with different curing treatments (non-carbonated and carbonated) before and after ageing. The different parameters are Modulus of Rupture (MOR), Specific Energy (SE), Specific Deflection (SD), Modulus of Elasticity (MOE), Limit of Proportionality (LOP), Apparent Porosity (AP), Bulk Density (BD) and Water Absorption (WA).

		MOR (MPa)				SE (kJ/m^2)				SD (mm/mm)			
		Unaged		Aged		Unaged		Aged		Unaged		Aged	
Non-carbonated	$\bar{x}$	12.22	a, A	12.30	a, A	7.67	a, A	10.27	a, A	0.112	a, A	0.152	a, B
	σ	0.53		1.36		1.48		2.21		0.02		0.02	
Carbonated	$\bar{x}$	13.24	a, A	13.84	a, A	8.07	a, A	8.79	a, A	0.105	b, A	0.107	b, A
	σ	1.55		1.87		3.12		3.91		0.03		0.04	

		MOE (GPa)				LOP (MPa)			
		Unaged		Aged		Unaged		Aged	
Non-carbonated	$\bar{x}$	3.418	a, A	5.529	a, B	7.31	a, A	4.76	a, B
	σ	0.29		0.99		0.87		1.07	
Carbonated	$\bar{x}$	8.679	b, A	11.55	b, B	8.72	b, A	10.47	b, B
	σ	1.00		1.67		1.14		1.18	

		AP (% by volume)				BD (g/cm^3)				WA (% by mass)			
		Unaged		Aged		Unaged		Aged		Unaged		Aged	
Non-carbonated	$\bar{x}$	36.95	a, A	37.39	a, A	1.48	a, A	1.45	a, A	25.02	a, A	25.83	a, A
	σ	0.79		1.12		0.03		0.03		1.00		1.34	
Carbonated	$\bar{x}$	30.72	b, A	26.78	b, B	1.62	b, A	1.69	b, B	18.94	b, A	15.84	b, B
	σ	1.11		1.01		0.03		0.03		0.88		0.99	

Same lower case letters in the same column mean no statistical significant difference.

Same capital letters in the same row mean no significant statistical significant difference.

Regarding the physical properties, carbonation has a beneficial effect since AP and WA are reduced for carbonated samples. The reduction of these parameters is higher after ageing and inversely proportional to the BD, which is greater for carbonated samples. This higher density is attributed to a more compact matrix that is the responsible of the better mechanical performance of the carbonated composites.

CONCLUSION

The curing treatment with higher CO_2 concentration in composites with MgO-based cements is associated to very desirable effects, since it improves both mechanical and physical properties of the composites. This improvement is attributed to the densening effect that carbonation reaction has on the matrix, where $Mg(OH)_2$ is transformed into bigger and denser particles of hydrated magnesium carbonates. The carbonation of $Mg(OH)_2$ is confirmed by XRD, since carbonated samples present diminished peaks related to this crystalline phase, while peaks associated to HMC are present. Also by thermogravimetry test, it is confirmed the presence HMC that are stable over time. SEM analysis also helps to detect these new crystalline phases that are coincident in shape with hydromagnesite crystals.

All these findings bring an innovative technology to use different types of cement to produce FC products. For that, further study is necessary in order to optimize and implement this solution. This clinker-free cement would allow the use of only cellulosic pulps with no degradation effects. In addition, the use of carbonation curing may additionally increase the properties of the composites with an improvement of the dimensional stability.

ACKNOWLEDGEMENTS

Authors are thankful to FAPESP (2012/51467-3), CNPq (307723/2017-8) and Capes.

REFERENCES

Almeida, A.E.F.S., Tonoli, G.H.D., Santos, S.F., Savastano Jr., H., 2013. Improved durability of vegetable fiber reinforced cement composite subject to accelerated carbonation at early age. Cem. Concr. Compos. 42, 49–58. https://doi.org/10.1016/j.cemconcomp.2013.05.001

ASTM C1185-08, 2012. Test Methods for Sampling and Testing Non-Asbestos Fiber-Cement Flat Sheet, Roofing and Siding Shingles, and Clapboards. ASTM International, West Conshohocken, PA, USA.

Beall, G.W., Duraia, E.-S.M., El-Tantawy, F., Al-Hazmi, F., Al-Ghamdi, A.A., 2013. Rapid fabrication of nanostructured magnesium hydroxide and hydromagnesite via microwave-assisted technique. Powder Technol. 234, 26–31. https://doi.org/10.1016/j.powtec.2012.09.029

Botha, A., Strydom, C.A., 2001. Preparation of a magnesium hydroxy carbonate from magnesium hydroxide. Hydrometallurgy 62, 175–183. https://doi.org/10.1016/S0304-386X(01)00197-9

Chen, L., Ye, G., Wang, Q., Blanpain, B., Malfliet, A., Guo, M., 2015. Low temperature synthesis of forsterite from hydromagnesite and fumed silica mixture. Ceram. Int. 41, 2234–2239. https://doi.org/10.1016/j.ceramint.2014.10.025

Frías, M., Goñi, S., 2013. Accelerated carbonation effect on behaviour of ternary Portland cements. Compos. Part B Eng. 48, 122–128. https://doi.org/10.1016/j.compositesb.2012.12.008

Gautier, Q., Bénézeth, P., Mavromatis, V., Schott, J., 2014. Hydromagnesite solubility product and growth kinetics in aqueous solution from 25 to 75°C. Geochim. Cosmochim. Acta 138, 1–20. https://doi.org/10.1016/j.gca.2014.03.044

Haurie, L., Fernandez, A.I., Velasco, J.I., Chimenos, J.M., Lopez-Cuesta, J.M., Espiell, F., 2007. Effects of milling on the thermal stability of synthetic hydromagnesite. Mater. Res. Bull. 42, 1010–1018. https://doi.org/10.1016/j.materresbull.2006.09.020

Hollingbery, L.A., Hull, T.R., 2012. The thermal decomposition of natural mixtures of huntite and hydromagnesite. Thermochim. Acta 528, 45–52. https://doi.org/10.1016/j.tca.2011.11.002

Hollingbery, L.A., Hull, T.R., 2010a. The fire retardant behaviour of huntite and hydromagnesite – A review. Polym. Degrad. Stab. 95, 2213–2225. https://doi.org/10.1016/j.polymdegradstab.2010.08.019

Hollingbery, L.A., Hull, T.R., 2010b. The thermal decomposition of huntite and hydromagnesite—A review. Thermochim. Acta 509, 1–11. https://doi.org/10.1016/j.tca.2010.06.012

Lanas, J., Alvarez, J.I., 2004. Dolomitic lime: thermal decomposition of nesquehonite. Thermochim. Acta 421, 123–132. https://doi.org/10.1016/j.tca.2004.04.007

Li, Q., Ding, Y., Yu, G., Li, C., Li, F., Qian, Y., 2003. Fabrication of light-emitting porous hydromagnesite with rosette-like architecture. Solid State Commun. 125, 117–120. https://doi.org/10.1016/S0038-1098(02)00710-X

Li, Z., Zhang, T., Hu, J., Tang, Y., Niu, Y., Wei, J., Yu, Q., 2014. Characterization of reaction products and reaction process of MgO–SiO2–H2O system at room temperature. Constr. Build. Mater. 61, 252–259. https://doi.org/10.1016/j.conbuildmat.2014.03.004

Lothenbach, B., Nied, D., L'Hôpital, E., Achiedo, G., Dauzères, A., 2015. Magnesium and calcium silicate hydrates. Cem. Concr. Res. 77, 60–68. https://doi.org/10.1016/j.cemconres.2015.06.007

Mármol, G., Savastano, H., 2017. Study of the degradation of non-conventional MgO-SiO 2 cement reinforced with lignocellulosic fibers. Cem. Concr. Compos. 80, 258–267. https://doi.org/10.1016/j.cemconcomp.2017.03.015

Mo, L., Zhang, F., Deng, M., 2015. Effects of carbonation treatment on the properties of hydrated fly ash-MgO-Portland cement blends. Constr. Build. Mater. 96, 147–154. https://doi.org/10.1016/j.conbuildmat.2015.07.193

Morandeau, A., Thiéry, M., Dangla, P., 2015. Impact of accelerated carbonation on OPC cement paste blended with fly ash. Cem. Concr. Res. 67, 226–236. https://doi.org/10.1016/j.cemconres.2014.10.003

Pizzol, V.D., Mendes, L.M., Savastano, H., Frías, M., Davila, F.J., Cincotto, M.A., John, V.M., Tonoli, G.H.D., 2014. Mineralogical and microstructural changes promoted by accelerated carbonation and ageing cycles of hybrid fiber–cement composites. Constr. Build. Mater. 68, 750–756. https://doi.org/10.1016/j.conbuildmat.2014.06.055

Purnell, P., Short, N.., Page, C.., 2001. Super-critical carbonation of glass-fibre reinforced cement. Part 1: mechanical testing and chemical analysis. Compos. Part Appl. Sci. Manuf. 32, 1777–1787. https://doi.org/10.1016/S1359-835X(01)00019-7

Santos, S.F., Schmidt, R., Almeida, A.E.F.S., Tonoli, G.H.D., Savastano, H., 2015. Supercritical carbonation treatment on extruded fibre–cement reinforced with vegetable fibres. Cem. Concr. Compos. 56, 84–94. https://doi.org/10.1016/j.cemconcomp.2014.11.007

Savastano Jr., H., Warden, P.., Coutts, R.S.., 2000. Brazilian waste fibres as reinforcement for cement-based composites. Cem. Concr. Compos. 22, 379–384. https://doi.org/10.1016/S0958-9465(00)00034-2

Szczerba, J., Prorok, R., Śnieżek, E., Madej, D., Maślona, K., 2013. Influence of time and temperature on ageing and phases synthesis in the MgO–SiO2–H2O system. Thermochim. Acta 567, 57–64. https://doi.org/10.1016/j.tca.2013.01.018

Unluer, C., Al-Tabbaa, A., 2015. The role of brucite, ground granulated blastfurnace slag, and magnesium silicates in the carbonation and performance of MgO cements. Constr. Build. Mater. 94, 629–643. https://doi.org/10.1016/j.conbuildmat.2015.07.105

Unluer, C., Al-Tabbaa, A., 2014. Enhancing the carbonation of MgO cement porous blocks through improved curing conditions. Cem. Concr. Res. 59, 55–65. https://doi.org/10.1016/j.cemconres.2014.02.005

Unluer, C., Al-Tabbaa, A., 2013. Impact of hydrated magnesium carbonate additives on the carbonation of reactive MgO cements. Cem. Concr. Res. 54, 87–97. https://doi.org/10.1016/j.cemconres.2013.08.009

Vágvölgyi, V., Frost, R.L., Hales, M., Locke, A., Kristóf, J., Horváth, E., 2008. Controlled rate thermal analysis of hydromagnesite. J. Therm. Anal. Calorim. 92, 893–897. https://doi.org/10.1007/s10973-007-8845-6

Vandeperre, L.J., Al-Tabbaa, A., 2007. Accelerated carbonation of reactive MgO cements. Adv. Cem. Res. 19, 67–79. https://doi.org/10.1680/adcr.2007.19.2.67

Walling, S.A., Kinoshita, H., Bernal, S.A., Collier, N.C., Provis, J.L., 2015. Structure and properties of binder gels formed in the system $Mg(OH)_2$ –SiO_2 –H_2O for immobilisation of Magnox sludge. Dalton Trans 44, 8126–8137. https://doi.org/10.1039/C5DT00877H

Zha, X., Yu, M., Ye, J., Feng, G., 2015. Numerical modeling of supercritical carbonation process in cement-based materials. Cem. Concr. Res. 72, 10–20. https://doi.org/10.1016/j.cemconres.2015.02.017